JOURNAL OF Materials CHEMISTRY

Photoinduced electron transfer in π-extended tetrathiafulvalene–porphyrin–fullerene triad molecules

Gerdenis Kodis, Paul A. Liddell, Linda de la Garza, Ana L. Moore,* Thomas A. Moore* and Devens Gust*

Department of Chemistry and Biochemistry, Center for the Study of Early Events in Photosynthesis, Arizona State University, Tempe, AZ 85287, USA. E-mail: Gust@asu.edu

Received 28th January 2002, Accepted 11th March 2002
First published as an Advance Article on the web 22nd April 2002

Two molecular triads consisting of a porphyrin (P) covalently linked to a fullerene electron acceptor (C_{60}) and a π-extended tetrathiafulvalene electron donor (TTF) have been synthesized. Time resolved spectroscopic investigations of the triad featuring a free base porphyrin moiety (TTF–P_{2H}–C_{60}) show that in 2-methyltetrahydrofuran solution, excitation of the porphyrin leads to formation of a TTF–$P_{2H}^{\bullet+}$–$C_{60}^{\bullet-}$ charge-separated state in 25 ps. Electron transfer from the TTF generates a final $TTF^{\bullet+}$–P_{2H}–$C_{60}^{\bullet-}$state with an overall yield of 0.87. This species decays to the ground state in 1.07 μs. Similar experiments on the zinc analog, TTF–P_{Zn}–C_{60}, show formation of TTF–$P_{Zn}^{\bullet+}$–$C_{60}^{\bullet-}$ in 1.5 ps, followed by generation of $TTF^{\bullet+}$–P_{Zn}–$C_{60}^{\bullet-}$ with a yield of 0.09. This charge-separated state also decays to the ground state in 1.07 μs. Comparison of these results with those for previously reported triads with different donor moieties reveals differences in electron transfer rate constants that can be qualitatively understood in the framework of the Marcus–Hush electron transfer formalism.

Introduction

As understanding of the natural photosynthetic process increases, it is becoming clear that photosynthesis can serve as a model for many fundamental and potentially technologically useful processes at the nanoscale. For example, the various photosynthetic antenna systems may be viewed as nanoscale photonic devices that perform transport and switching operations with excitation energy. Reaction centers are molecular-scale photovoltaics that use light energy to generate energetic charge-separated states. Research in artificial photosynthesis—mimicry of the process with synthetic systems—has advanced dramatically over the last 20 years.[1–5] This progress opens the door not only to the design of artificial constructs that convert light energy into biologically useful forms, but also to the preparation of molecular scale electronic and optoelectronic devices that may ultimately be useful in computing and communications.[6]

Artificial photosynthetic reaction centers are based upon photoinduced electron transfer, whereby an excited state of a chromophore relaxes by charge donation to a nearby acceptor. If the resulting charge-separated state is energetic, long-lived, and produced in high yield, it can be suitable for exploitation by additional, energy-requiring processes. Since our initial report of photoinduced electron transfer in a molecular dyad consisting of a fullerene covalently linked to a synthetic porphyrin,[7] fullerenes have been found to be excellent electron acceptor moieties for incorporation into multicomponent ''supermolecules'' that act as artificial reaction centers. There are several reasons for this. Functionalized C_{60} molecules have first reduction potentials similar to those of quinones (which are biological redox couples), and reversibly accept up to six electrons. They absorb light over much of the visible spectrum. Flexible methodologies for fullerene modification permit their incorporation into a variety of structures. Importantly, they have been found to have small internal and solvent reorganization energies, and low sensitivity to solvent stabilization of their anions.[8–14] These features lead to desirable electron transfer properties such as rapid photoinduced electron transfer and slow charge recombination.

A recent example of a fullerene-containing artificial reaction center is molecular triad **1**, which contains a porphyrin chromophore, P, covalently linked to a fullerene electron acceptor, C_{60}, and a tetrathiafulvalene electron donor, TTF.[15] The tetrathiafulvalene electron donor moiety has recently been paired with fullerenes in a variety of potential molecular device applications.[16–29] Transient spectroscopic studies demonstrated that excitation of the porphyrin moiety in 2-methyltetrahydrofuran solution yielded its first excited singlet state TTF–$^1P_{2H}$–C_{60}, which decayed in 25 ps by photoinduced electron transfer to the fullerene to give the TTF–$P_{2H}^{\bullet+}$–$C_{60}^{\bullet-}$ charge-separated state with a quantum yield of 1.0. Competing with charge recombination was donation of an electron from the TTF moiety to yield a final $TTF^{\bullet+}$–P_{2H}–$C_{60}^{\bullet-}$ charge-separated state. This state was formed with a yield of 92% and decayed to the ground state in 660 ns. Similar photochemistry (with different rate constants) was observed for zinc-containing analog **2**.

The fact that fullerenes can act as multiple electron acceptors suggests that sequential two-photon excitation of suitable molecular photovoltaic compounds might lead to interesting photoinduced electron transfer behavior and perhaps charge accumulation. However, energetic considerations suggest that such behavior is unlikely for **1** or **2** (Fig. 1). The excited state of the free base porphyrin moiety of **1** is not energetic enough to either donate an electron to the fullerene radical anion or accept an electron from the TTF radical cation. The first excited singlet state of the zinc porphyrin of **2** is thermodynamically capable of electron donation to the fullerene radical anion, but the resulting zinc porphyrin radical cation is not capable of oxidizing the TTF radical cation to give a long-lived TTF^{++}–P–C_{60}^{2-} state. Various π-extended tetrathiafulvalenes have the interesting characteristic that the first and second oxidation potentials are similar, or in some cases nearly identical. In a triad analogous to **1** or **2** bearing such a donor, transfer of a second electron from the TTF to a porphyrin first excited singlet state or radical cation might be energetically possible, giving rise to novel photochemistry. With this in mind, we have prepared triads **3** and **4**, each of which features a π-extended TTF group. Here, we report the synthesis of these

 DOI: 10.1039/b201039a

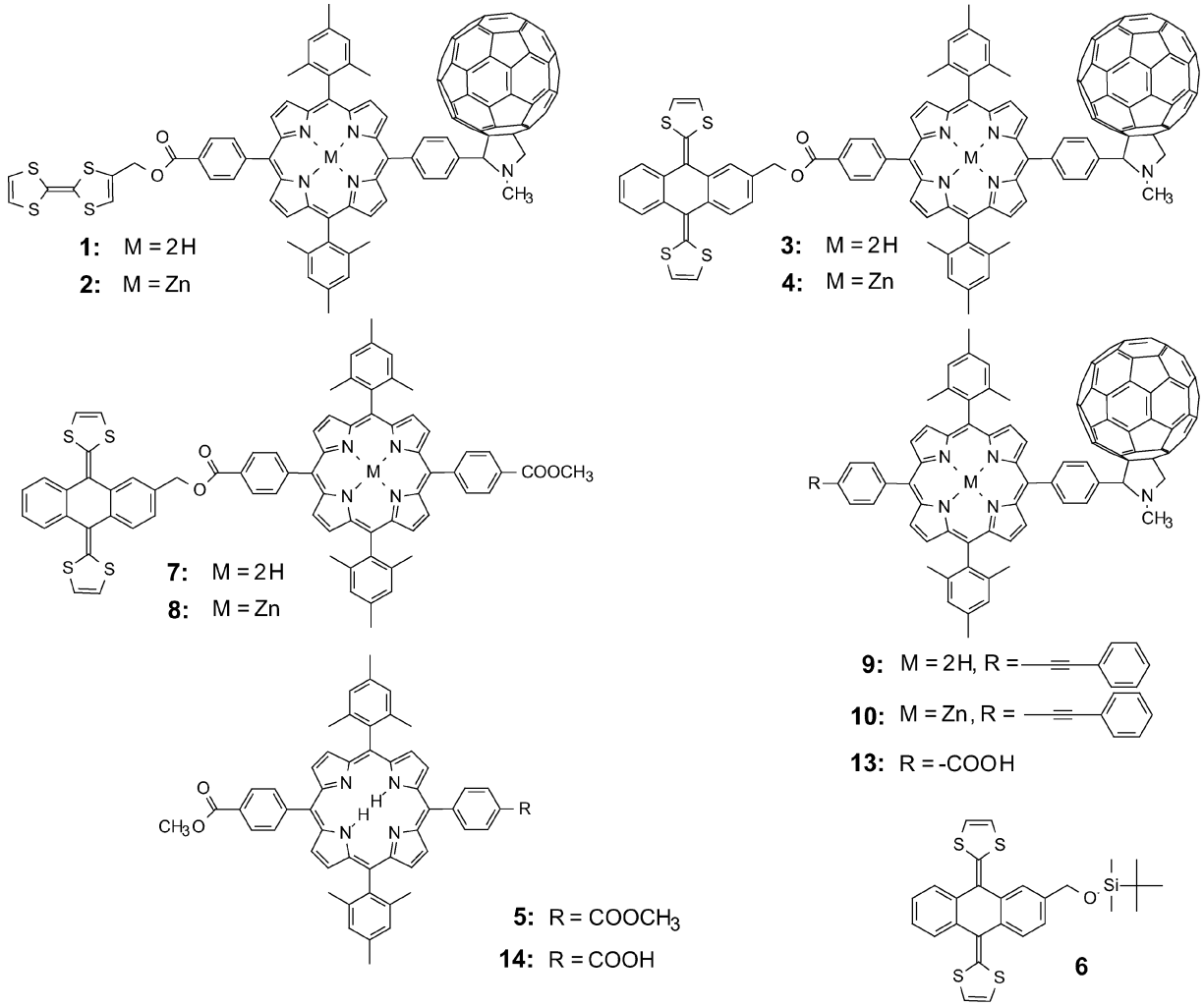

Fig. 1 Structures of the triads, model compounds and precursors.

compounds and the results of studies of the photochemistry following single-photon excitation.

Results

Synthesis

The porphyrin–fullerene dyad portion of triads **3** and **4** was prepared by a route similar to that reported earlier[15] for **1** and **2**. One of the ester groups of porphyrin **5** was converted to an aldehyde *via* reduction with lithium aluminium hydride followed by oxidation of the resulting benzylic alcohol with manganese dioxide. Reaction[30] of the aldehyde with sarcosine and C_{60} gave a porphyrin–fullerene dyad. The remaining ester moiety was treated with boron tribromide to generate acid **13**. The π-extended TTF species **6** was prepared using a method related to that employed by Bryce and coworkers for the synthesis of a methylthio-substituted π-extended TTF derivative bearing a hydroxymethyl group.[31] Deprotection of **6** with tetrabutylammonium fluoride and coupling with acid **13** gave triad **3**, which was metalated with zinc acetate to yield **4**. Synthetic details and analytical data are provided in the Experimental section.

Cyclic voltammetry

Electrochemical measurements were undertaken to investigate the redox properties of TTF model **6** and the triads **3** and **4**. These were necessary in order to estimate the energies of charge-separated states. The measurements were carried out with a Pine Instrument Co. Model AFRDE4 potentiostat at ambient temperatures with a glassy carbon working electrode, a Ag/Ag^+ reference electrode, and a platinum wire counter electrode. Measurements were performed in benzonitrile containing 0.1 M tetra-*n*-butylammonium hexafluorophosphate, and ferrocene as an internal redox standard (oxidation at 0.46 V *vs.* SCE). Compound **6** featured a quasireversible oxidation wave with a peak at 0.46 V *vs.* SCE. Similar behavior has been observed for the parent π-extended TTF, and the oxidation shown to be a 2-electron process, corresponding to the first two oxidations of the TTF.[29,32,33] Free-base triad **3** showed a similar quasireversible TTF oxidation at 0.48 V, the first oxidation of the free base porphyrin ring at 1.02 V, and reduction at −0.56, −0.97 and −1.17 V *vs.* SCE. The first two reduction waves are due to the fullerene moiety, and the third to the free-base porphyrin.[34] Zinc-containing triad **4** demonstrated a two-electron quasireversible oxidation of TTF at 0.50 V, and the first oxidation of the porphyrin at 0.82 V. Fullerene reductions were at −0.56 and −1.00 V. The potentials measured for the triads are all very similar to those measured for model porphyrins and fullerenes, indicating that linking the moieties in the triad does little to perturb the individual redox centers.

Absorption spectra

The absorption spectrum of free-base triad **3** in 2-methyltetrahydrofuran is shown in Fig. 2a. The maxima are at ~255, 362, 415, 482, 514, 548, 591, 648, and 705 nm (very weak). Similarly, the absorption spectrum of zinc triad **4** (Fig. 2b)

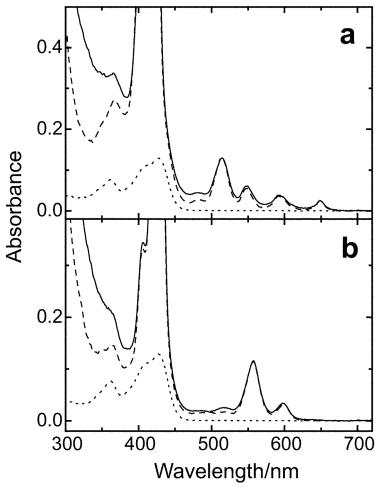

Fig. 2 Absorption spectra in 2-methyltetrahydrofuran of (a) TTF–P_{2H}–C_{60} triad **3** (—), TTF–P_{2H} dyad **7** (– – –), and TTF model compound **6** (···). The spectra for the porphyrin-containing moieties have been normalized at the long-wavelength Q-band absorption at 658 nm; (b) TTF–P_{Zn}–C_{60} triad **4** (—), TTF–P_{Zn} dyad **8** (– – –), and TTF model compound **6** (···). The spectra for the porphyrin-containing moieties have been normalized at the long-wavelength Q-band absorption at 598 nm.

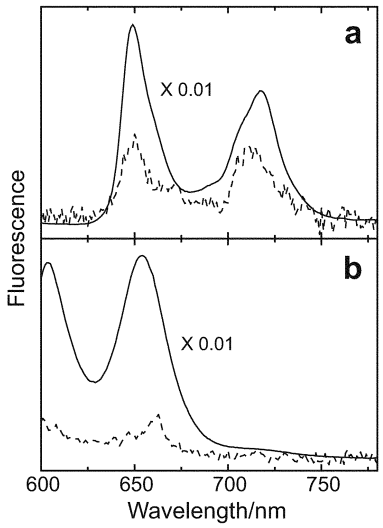

Fig. 3 Corrected fluorescence emission spectra obtained in 2-methyltetrahydrofuran solution with excitation at 590 nm. (a) TTF–P_{2H} dyad **7** (—) and TTF–P_{2H}–C_{60} triad **3** (– – –). The samples had the same absorbance at 590 nm, and the emission spectrum of **7** has been multiplied by 0.01 to facilitate comparison. (b) TTF–P_{Zn} dyad **8** (—) and TTF–P_{Zn}–C_{60} triad **4** (– – –). The samples had the same absorbance at 590 nm, and the emission spectrum of **8** has been multiplied by 0.01 to facilitate comparison.

shows maxima at ~255, 362, 405(sh), 420, 518, 557, 598, and 705 nm (very weak). The absorption maximum at 362 nm in both compounds is ascribed to the π-extended tetrathiafulvalene moiety, as demonstrated by the absorption spectrum of model compound **6**, which has bands at 362, 410 and 428 nm. In both triads, the bands at ~255 and 705 nm, with continuous weak absorption at intermediate wavelengths, are characteristic of the fullerene. The remaining major bands in the spectra are assigned to the porphyrin moieties, by reference to spectra of model porphyrins such as **5**.

For comparison, Fig. 2 also shows the spectra of model tetrathiafulvalene–porphyrin dyads **7** and **8**, normalized to the spectra of **3** and **4**, respectively, at either 648 nm (free-base porphyrin) or 598 nm (zinc porphyrin). Subtraction of the absorption spectrum of **7** from that of **3**, or **8** from **4**, yields a spectrum characteristic of a fullerene with a substitution pattern similar to that of the fullerene moiety in these compounds. In fact, the absorption spectra of the triads are essentially linear combinations of the spectra of TTF, porphyrin, and fullerene model compounds, and show no significant perturbations indicative of strong interactions between the linked moieties. With excitation at 650 nm, it is possible to excite the free-base porphyrin of **3** almost exclusively. Similarly, excitation of **4** at 600 nm will produce almost exclusively the zinc porphyrin first excited singlet state.

Fluorescence emission spectra

The fluorescence spectra of triad **3** and dyad **7** in 2-methyltetrahydrofuran, obtained with equal absorbance at the excitation wavelength of 590 nm, are shown in Fig. 3a. The porphyrin emission for the TTF–P_{2H}–C_{60} triad is quenched by a factor of 200, relative to the emission of the TTF–P_{2H} dyad. Quenching is also seen for the zinc triad, whose emission in 2-methyltetrahydrofuran is shown in Fig. 3b. The emission of **4** is characteristic of a zinc porphyrin, with maxima at ~603 and ~654. However, it is weaker than that of model dyad **8** by a factor of 650. By analogy with previously reported porphyrin–fullerene dyads, we ascribe this quenching to photoinduced electron transfer from the porphyrin to the fullerene. As shown below, this assumption is verified by additional spectroscopic studies.

Time-resolved fluorescence

The very strong fluorescence quenching observed for **3** and **4** allows the possibility that the steady-state fluorescence emission that is observed in these compounds may be due to very minor, but strongly fluorescent, impurities, rather than the triads themselves. We turned to time resolved fluorescence techniques in order to obtain more relevant data. Fig. 4 shows typical fluorescence decays obtained using the single photon timing technique, and determined in deaerated 2-methyltetrahydrofuran solution with excitation at 590 nm and detection at 650 nm, where both free-base and zinc porphyrin moieties emit.

As illustrated in Fig. 4, the fluorescence decay of TTF–free-base porphyrin dyad **7** could be fitted as a single exponential process with a lifetime of 8.6 ns (χ^2 = 1.03). This lifetime indicates a slight quenching of the 11.0 ns lifetime typical for porphyrins of this general type.[35] The quenching is ascribed to photoinduced electron transfer from the TTF moiety to form a $TTF^{\bullet+}$–$P_{2H}{}^{\bullet-}$ charge-separated state. The decay from TTF–P_{2H}–C_{60} triad **3** was fitted as four exponential decays with lifetimes of 29 ps, 157 ps, 878 ps and 6.7 ns (χ^2 = 1.06). The latter three components made up ⩽6% of the total amplitude, and are ascribed to minor impurities or fitting artifacts. The

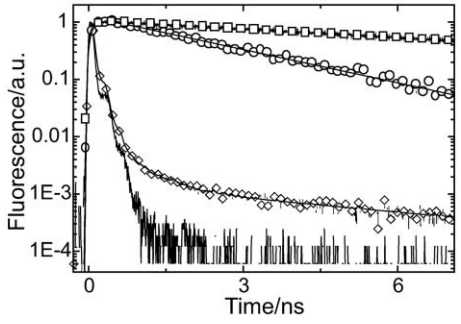

Fig. 4 Fluorescence decays in 2-methyltetrahydrofuran solution with excitation at 590 nm and detection at 650 nm: TTF–P_{2H}–C_{60} triad **3** (◊), TTF–P_{2H} dyad **7** (□), TTF–P_{Zn} dyad **8** (○), and instrument response function (—). The solid lines through the data points for the three compounds are the best theoretical fits to the data, and yield the time constants reported in the text. Note the log scale for fluorescence intensity.

29 ps component is due to strong quenching of the porphyrin first excited singlet state by the fullerene, which is consistent with the steady-state results reported above.

The fluorescence decay of TTF–P_{Zn} dyad **8** was fitted as a single exponential process with a time constant of 2.2 ns ($\chi^2 = 1.19$). This lifetime is similar to that of model zinc porphyrins of this general type, and indicates no significant quenching of the porphyrin first excited singlet state by the TTF moiety. With TTF–P_{Zn}–C_{60} triad **4**, no significant fluorescence emission was observed. This suggests that the lifetime of the zinc porphyrin first excited singlet state is shorter than the time resolution of the spectrometer ($\sim$5 ps).

Time-resolved absorption

Transient absorption experiments were undertaken in order to better quantify the formation and decay of the various transient states. Solutions ($\sim 1 \times 10^{-3}$ M) in 2-methyltetrahydrofuran were excited with $\sim$100 fs laser pulses and the transient absorption spectra were recorded using the pump–probe method. Excitation was at 650 and/or 600 nm. Spectra were recorded in the 930–1070 nm and 450–760 nm regions, at times ranging from -50 to 4500 ps relative to the laser flash. Data were fitted globally using singular value decomposition methods.[36,37]

Free-base porphyrin systems. It was postulated above that quenching of the first excited singlet state of the free-base porphyrin of triad **3** was due to photoinduced electron transfer to the fullerene. Support for this conclusion comes from a previously reported study of porphyrin–fullerene dyad **9** in 2-methyltetrahydrofuran.[35] The sample was excited at 650 nm, where most of the light is absorbed by the porphyrin. Immediately after excitation, absorptions characteristic of $^1P_{2H}$–C_{60} were observed. The singlet evolved into the $P_{2H}^{\bullet+}$–$C_{60}^{\bullet-}$ charge-separated state with a time constant of 25 ps. The charge-separated state decayed to the ground state with a lifetime of 3.0 ns. Transient absorption studies at several wavelengths showed that excitation of the porphyrin moiety does not lead to significant population of the fullerene first excited singlet state by singlet–singlet energy transfer; photoinduced electron transfer is the only important decay pathway for $^1P_{2H}$–C_{60}.[35]

Fig. 5a shows results obtained from excitation of triad **3** in 2-methyltetrahydrofuran solution with a 600 nm laser pulse. This light is absorbed mainly by the porphyrin moiety, generating TTF–$^1P_{2H}$–C_{60}. Over time, a new transient grows in with an absorbance maximum at $\sim$1000 nm (inset in Fig. 5a). This is due to the fullerene radical anion. When the spectrum is monitored at 1000 nm, the radical anion absorption is found to rise with a time constant of 25 ps, which corresponds, within experimental error, to the decay time for the porphyrin first excited singlet state as determined by the time-resolved fluorescence studies (29 ps), and to the rise time of $P_{2H}^{\bullet+}$–$C_{60}^{\bullet-}$ in dyad **9** (25 ps). The fullerene radical anion absorption band does not decay over a period of 4 ns, which is the longest time scale available on the spectrometer.

Fig. 6a shows decay-associated spectra for triad **3** determined by global analysis of transient absorption data obtained with excitation of the porphyrin at 650 nm. The best theoretical fit to the data set was achieved with three components: 25 ps, 380 ps, and a component that did not decay on this time scale. The 25 ps component has bleaching bands at $\sim$515, $\sim$550, $\sim$590, and $\sim$650 nm, and negative amplitude in the red part of spectrum corresponding to stimulated emission bands at $\sim$650 and $\sim$720 nm. These are all characteristic of the free-base porphyrin, and are assigned to decay of the porphyrin first excited singlet state and concomitant formation of the porphyrin radical cation with absorption in 600–800 nm region. This result is

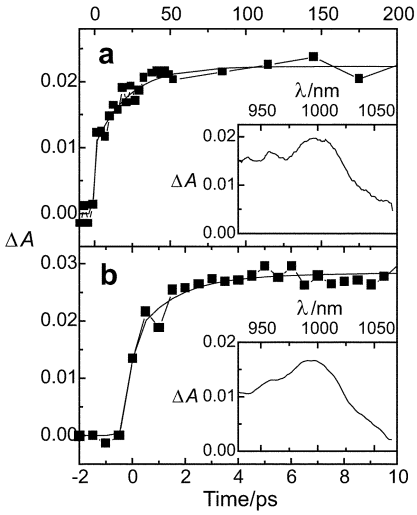

Fig. 5 (a) Transient absorption at 1000 nm of a 2-methyltetrahydrofuran solution of TTF–P_{2H}–C_{60} triad **3** following excitation at 600 nm with a $\sim$100 fs laser pulse. The data, measured in the 1000 nm region, show the rise of the fullerene radical anion of TTF–$P_{2H}^{\bullet+}$–$C_{60}^{\bullet-}$ with a time constant of 25 ps (fit shown as a solid line). The inset shows the spectrum 500 ps after excitation; the anion transient absorption does not decay on this time scale. (b) Transient absorption at 1000 nm of a 2-methyltetrahydrofuran solution of TTF–P_{Zn}–C_{60} triad **4** following excitation at 600 nm with a $\sim$100 fs laser pulse. The data, measured in the 1000 nm region, show the rise of the fullerene radical anion of TTF–$P_{Zn}^{\bullet+}$–$C_{60}^{\bullet-}$ with a time constant of 1.5 ps (fit shown as a solid line). The inset shows the spectrum 500 ps after excitation; the anion transient absorption does not decay on this time scale.

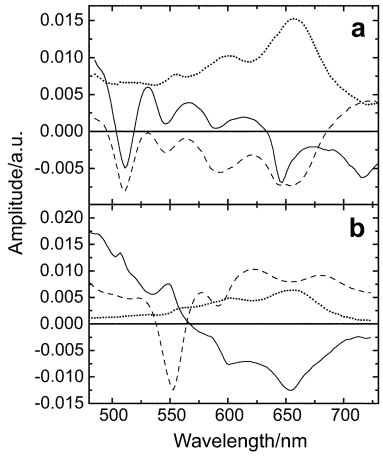

Fig. 6 (a) Decay-associated spectra for free-base triad **3** determined by global analysis of transient absorption data obtained with excitation of a 2-methyltetrahydrofuran solution at 650 nm. Two components have time constants of 25 ps (—) and 380 ps (– – –), and the third is non-decaying on this time scale (···). (b) Decay-associated spectra for zinc triad **4** determined by global analysis of transient absorption data obtained with excitation of a 2-methyltetrahydrofuran solution at 600 nm. Two components have time constants of 1.5 ps (—) and 610 ps (– – –), and the third is non-decaying on this time scale (···).

indicative of formation of the TTF–$P_{2H}^{\bullet+}$–$C_{60}^{\bullet-}$ charge-separated state by photoinduced electron transfer.

The 380 ps component is mostly of negative amplitude. It has bleaching bands at $\sim$515, $\sim$550, $\sim$590, $\sim$650 nm and a broad induced absorption band at $\sim$700 nm, characteristic of the free base porphyrin radical cation. There is also an additional broad negative band around 655 nm. Negative amplitude there indicates the disappearance of the porphyrin bleaching bands with time and the rise of a new transient species that does not have bleaching at these wavelengths. We ascribe the 380 ps component to decay of TTF–$P_{2H}^{\bullet+}$–$C_{60}^{\bullet-}$ by charge shift to the TTF moiety, leading to formation of a TTF$^{\bullet+}$–P_{2H}–$C_{60}^{\bullet-}$

charge-separated state. The spectrum of the non-decaying component is consistent with that of the π-extended tetrathiafulvalene radical cation, with absorption maxima at ~655, 600 and 505 nm.[38]

Zinc porphyrin systems. Zinc dyad **10** has been previously investigated using the pump–probe technique with excitation at 600 nm, where most of the absorption is by the zinc porphyrin.[15] Excitation produced the porphyrin first excited singlet state $^1P_{Zn}$–C_{60}, which rapidly evolved into the $P_{Zn}^{\bullet+}$–$C_{60}^{\bullet-}$ charge-separated state with a time constant of 1.5 ps. The charge-separated state decayed to the ground state with a lifetime of 680 ps.

Turning to triad **4**, similar transient absorption experiments with excitation at 600 nm showed that the laser flash yielded TTF–$^1P_{Zn}$–C_{60}, which decayed to give the TTF–$P_{Zn}^{\bullet+}$–$C_{60}^{\bullet-}$ charge-separated state with a time constant of 1.5 ps (Fig. 5b). The fullerene radical anion absorption in the 1000 nm region, which did not decay on the time scale of the measurement, is shown in the inset. Decay-associated spectra for **4** are shown in Fig. 6b, and feature components with lifetimes of 1.5 ps and 610 ps, plus a component that does not decay on this time scale.

The 1.5 ps component has bands at ~515, ~560, ~600 and ~650 nm that are characteristic of the zinc porphyrin. The negative amplitude in the longer-wavelength portion of the spectrum (stimulated emission bands at ~600 and ~650 nm) and the positive amplitude in the shorter-wavelength portion of the spectrum are indicative of the decay of the porphyrin first excited singlet state and the concomitant formation of the zinc porphyrin radical cation. These results confirm the formation of TTF–$P_{Zn}^{\bullet+}$–$C_{60}^{\bullet-}$. Charge separation is very fast, and comparable with the solvation time of the porphyrin excited singlet state. Examination of individual spectra at various times reveals that the porphyrin bleaching bands at ~515 and ~560 nm initially appear to the blue of these wavelengths, and move to the red as the spectrum evolves. For this reason, the decay-associated spectrum in Fig. 6b reflects both the initial appearance of the porphyrin bleaching bands at the shorter wavelengths and their movement to the red during their formation.

The 610 ps component is mostly of positive amplitude on the longer-wavelength side of the spectrum and has bleaching bands at shorter wavelengths. There is negative amplitude at the maximum of the ~560 nm bleaching band, indicating a rise of transient absorption that does not show bleaching at that wavelength. There is also a broad minimum at ~650 nm, indicating formation of a new transient with an absorption maximum at this wavelength. All this shows decay of TTF–$P_{Zn}^{\bullet+}$–$C_{60}^{\bullet-}$ and concomitant formation of the $TTF^{\bullet+}$–P_{Zn}–$C_{60}^{\bullet-}$ charge-separated state by a charge-shift. The long-lived component that does not decay on this time scale has a spectrum consistent with the π-extended tetrathiafulvalene radical cation and fullerene radical anion, as expected for the final $TTF^{\bullet+}$–P_{Zn}–$C_{60}^{\bullet-}$ species.

Lifetime of the charge-separated state. The lifetimes of the final charge-separated states in triads **3** and **4** are too long to be measured using the pump–probe technique, and appear as non-decaying spectral components in Fig. 5 and 6. We turned to nanosecond flash photolysis to determine their decay properties. Deoxygenated samples of **3** and **4** in 2-methyltetrahydrofuran were excited with ~5 ns laser pulses at 590 nm and the resulting spectral changes measured. Fig. 7 shows the resulting kinetic traces. Two of them, each featuring a decay time of 1.07 μs, were determined at 1000 nm and report on the decay of fullerene radical anion absorption. The other two, measured at 650 nm, reflect the absorption of the TTF radical cation and were also fitted as an exponential process with a time constant of 1.07 μs. Thus, $TTF^{\bullet+}$–P_{2H}–$C_{60}^{\bullet-}$ and $TTF^{\bullet+}$–P_{Zn}–$C_{60}^{\bullet-}$ each decay with a lifetime of 1.07 μs.

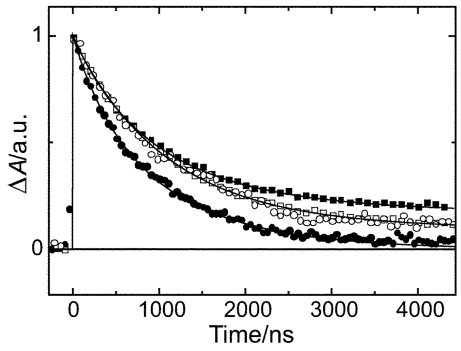

Fig. 7 Decay of the fullerene radical anion absorption measured at 1000 nm (open symbols) and the TTF radical cation absorption at 650 nm (filled symbols) determined after excitation of a 2-methyltetrahydrofuran solution of free-base porphyrin triad **3** (□,■) and zinc porphyrin triad **4** (○,●) with a ~5 ns laser pulse at 590 nm. Also shown are exponential fits to the data (solid lines).

Excitation of **3** and **4** produces a small amount of porphyrin and fullerene triplet states due to intersystem crossing. Therefore satisfactory fits of the decays required additional minor components (365 ns and tens of microseconds).

Discussion

Energetics

The transient spectral data for **3** and **4** will be discussed in terms of the kinetic schemes shown in Fig. 8. The energies of the excited singlet states are estimated as the wavenumber average of the longest-wavelength absorption and shortest-wavelength emission maxima of the triads and appropriate model compounds. The free-base porphyrin first excited singlet state lies 1.90 eV above the ground state, whereas the corresponding zinc porphyrin excited state is at 2.06 eV. The fullerene first excited singlet state is at 1.75 eV, and previous results have shown that in dyad **9**, direct excitation of this state is followed by photoinduced electron transfer to yield $P_{2H}^{\bullet+}$–$C_{60}^{\bullet-}$.[35] However, in the experiments described here, the fullerene first excited singlet state was not significantly populated either by direct excitation or by energy transfer, and so it is not indicated

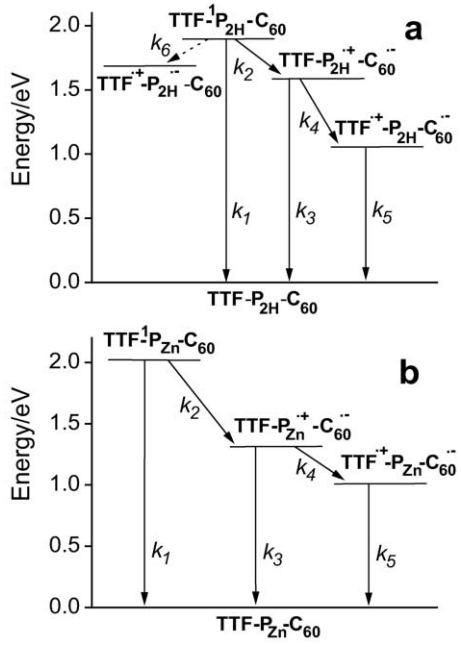

Fig. 8 Relevant transient states for triads **3** (a) and **4** (b), and interconversion pathways. Each reaction step (*e.g.*, step 2) is labeled with its corresponding rate constant (*e.g.*, k_2).

Table 1 Rate constants, quantum yields and free energy change values for triads **1**–**4** in 2-methyltetrahydrofuran

Cmpd	k_2/s^{-1}	Φ_2	ΔG^0_2/eV	k_3/s^{-1}	ΔG^0_3/eV	k_4/s^{-1}	Φ_4	ΔG^0_4/eV	k_5/s^{-1}	ΔG^0_5/eV	k_6/s^{-1}
1	4.0×10^{10}	1.0	−0.32	3.3×10^8	−1.58	4.0×10^9	0.92	−0.60	1.5×10^6	−0.98	6.3×10^7
2	6.7×10^{11}	1.0	−0.68	1.5×10^9	−1.38	2.8×10^8	0.16	−0.40	1.5×10^6	−0.98	–
3	4.0×10^{10}	1.0	−0.32	3.3×10^8	−1.58	2.3×10^9	0.87	−0.54	9.4×10^5	−1.04	2.5×10^7
4	6.7×10^{11}	1.0	−0.68	1.5×10^9	−1.38	1.4×10^8	0.09	−0.34	9.4×10^5	−1.04	–

in Fig. 8. Using a value of 0.48 V *vs.* SCE for the first oxidation potential of the TTF moiety in **3** and **4** in conjunction with the other electrochemical results described above, the energies of the TTF–$P_{2H}^{\bullet+}$–$C_{60}^{\bullet-}$, TTF–$P_{Zn}^{\bullet+}$–$C_{60}^{\bullet-}$, $TTF^{\bullet+}$–P_{2H}–$C_{60}^{\bullet-}$, $TTF^{\bullet+}$–P_{Zn}–$C_{60}^{\bullet-}$ and $TTF^{\bullet+}$–$P_{2H}^{\bullet-}$–C_{60} charge-separated states are estimated as 1.58, 1.38, 1.04, 1.04, and 1.65 eV, respectively. These estimates are not corrected for any coulombic effects that may be present. Table 1 lists the free energy change values for the various electron transfer events shown in Fig. 8. Also listed are corresponding values for triads **1** and **2**. The redox potential measurements suffer, of course, from experimental error, and from small ambiguities resulting from overlap of redox waves in the cyclic voltammograms. In order to facilitate comparison of all four triads, the values listed in the table assume that redox potentials differ for the two kinds of TTF moieties, as measured, but are identical to those reported above for identical porphyrin and fullerene moieties in the two sets of compounds.

Kinetic processes–free-base triad 3

The porphyrin first excited singlet state in **3** decays in part by the usual photophysical processes of intersystem crossing to the triplet, fluorescence and internal conversion. The sum of the rate constants for these processes, shown as k_1 in Fig. 8a, is $9.1 \times 10^7\ s^{-1}$, based on the 11.0 ns lifetime of model free-base porphyrins. In principle, this state could also decay by singlet–singlet energy transfer to the fullerene, or by electron transfer from the TTF moiety or to the fullerene. As mentioned above, singlet–singlet energy transfer was not observed. The TTF–$^1P_{2H}$ state in dyad **7** has a lifetime of 8.6 ns, and is thus only slightly quenched relative to model porphyrins. This quenching is attributed to photoinduced electron transfer from the TTF moiety to yield the $TTF^{\bullet+}$–$P_{2H}^{\bullet-}$ charge-separated state (analogous to step 6 in Fig. 8a). From these results, the value of k_6 for the similar process in triad **3** may be estimated using eqn. (1), where τ_f is the observed lifetime of the excited singlet state in **7** (8.6 ns). Thus, k_6 is $2.5 \times 10^7\ s^{-1}$ (corresponding to a quantum yield for charge separation of 0.21 in **7**).

$$1/\tau_f = k_1 + k_6 \quad (1)$$

In triad **3**, the lifetime of TTF–$^1P_{2H}$–C_{60} is only 25 ps, indicating that by far the major pathway for decay of the porphyrin excited singlet state is photoinduced electron transfer to the fullerene to generate TTF–$P_{2H}^{\bullet+}$–$C_{60}^{\bullet-}$ (step 2 in Fig. 8a). Eqn. (2) yields a value for k_2 of $4.0 \times 10^{10}\ s^{-1}$, giving a quantum yield for the initial charge-separated state, Φ_{in}, equal to 1.0.

$$1/\tau_f = k_1 + k_2 + k_6 \quad (2)$$

The TTF–$P_{2H}^{\bullet+}$–$C_{60}^{\bullet-}$ state may recombine to give the ground state (step 3), or evolve by electron transfer from the TTF moiety to the porphyrin radical cation, yielding the final $TTF^{\bullet+}$–P_{2H}–$C_{60}^{\bullet-}$ charge-separated state (step 4). The reciprocal of the 380 ps time constant observed for the decay of TTF–$P_{2H}^{\bullet+}$–$C_{60}^{\bullet-}$ and rise of $TTF^{\bullet+}$–P_{2H}–$C_{60}^{\bullet-}$ is the sum of the rate constants for these processes, k_3 and k_4. A value of $3.3 \times 10^8\ s^{-1}$ for k_3 may be estimated from the 3.0 ns lifetime of the $P_{2H}^{\bullet+}$–$C_{60}^{\bullet-}$ state of dyad **9**, giving a value for k_4 of $2.3 \times 10^9\ s^{-1}$. The yield of $TTF^{\bullet+}$–P_{2H}–$C_{60}^{\bullet-}$, Φ_{fi}, is given by eqn. (3),

$$\Phi_{fi} = \Phi_{in}((k_4/(k_3 + k_4)) \quad (3)$$

and equals 0.87. The $TTF^{\bullet+}$–P_{2H}–$C_{60}^{\bullet-}$ state decays to the ground state with a rate constant k_5 of $9.4 \times 10^5\ s^{-1}$, based on the 1.07 μs lifetime observed in the nanosecond transient absorption experiments.

Kinetic processes—zinc triad 4

The relevant states are shown in Fig. 8b. A value for k_1 of $4.6 \times 10^8\ s^{-1}$ may be estimated from the 2.2 ns lifetime of TTF–$^1P_{Zn}$ in dyad **8**. This lifetime is similar to that of excited singlet states in zinc porphyrin model compounds, demonstrating that TTF–$^1P_{Zn}$ is not quenched by electron transfer from the TTF moiety. This is not surprising, even though quenching was noted for free-base dyad **2a**. The driving force for the process is much reduced in the zinc triad, relative to **3**, because reduction potentials for zinc porphyrins are several hundred mV more negative than those for the corresponding free base. In addition, the unperturbed excited state lifetime of the zinc porphyrin is significantly shorter than that for the free base, limiting the effect of alternative decay pathways.

Given a value for k_1, the rate constant for photoinduced electron transfer, k_2, may be calculated from the 1.5 ps lifetime of TTF–$^1P_{Zn}$–C_{60} that was determined from the pump–probe transient absorption measurements: $k_2 = (1/1.5 \times 10^{-12}\ s) - 4.6 \times 10^8\ s^{-1} = 6.7 \times 10^{11}\ s^{-1}$. The rate constant for decay of TTF–$P_{Zn}^{\bullet+}$–$C_{60}^{\bullet-}$, k_3, is taken as the reciprocal of the 680 ps lifetime of $P_{Zn}^{\bullet+}$–$C_{60}^{\bullet-}$ in dyad **10**, or $1.5 \times 10^9\ s^{-1}$. The transient absorption experiments for **4** gave a time constant of 610 ps for formation of $TTF^{\bullet+}$–P_{Zn}–$C_{60}^{\bullet-}$ from TTF–$P_{Zn}^{\bullet+}$–$C_{60}^{\bullet-}$. Given these values, k_4, the rate constant for the charge-shift reaction in **4**, is found to be $1.4 \times 10^8\ s^{-1}$. The quantum yield of TTF-$P_{Zn}^{\bullet+}$–$C_{60}^{\bullet-}$ is 1.0, whereas that of the final $TTF^{\bullet+}$–P_{Zn}–$C_{60}^{\bullet-}$ species is 0.09. The rate constant for decay of $TTF^{\bullet+}$–P_{Zn}–$C_{60}^{\bullet-}$ to the ground state, k_5, equals $9.4 \times 10^5\ s^{-1}$, as determined from the 1.07 μs lifetime of the state.

Rate constants, quantum yields and thermodynamic driving force values for the various electron transfer steps in **1**–**4** are summarized in Table 1.

Comparison of free base and zinc triads

It is interesting to contrast the properties of the free-base and zinc triads with one another. With free-base triad **3**, photoinduced electron transfer to the fullerene (step 2 in Fig. 8a) dominates the other decay pathways, and gives the TTF–$P_{2H}^{\bullet+}$–$C_{60}^{\bullet-}$ state with a yield of unity. Photoinduced electron transfer by step 6 to yield $TTF^{\bullet+}$–$P_{2H}^{\bullet-}$–C_{60} has less thermodynamic driving force than step 2, and the electronic coupling between the donor and acceptor is likely smaller, given the greater number of single bonds in the linkage joining the moieties. It is also likely that the low solvent and internal reorganization energies (λ_s and λ_i) for electron transfer characteristic of the fullerene move step 2 toward the maximum of the Marcus–Hush relationship,[39–42] where $-\Delta G^\circ = \lambda$, thereby increasing the rate. The free energy change for step 6 in zinc triad **4** is significantly smaller than for the comparable step

in **3**, and electron transfer by this pathway is not observed. In the case of zinc-containing triad **4**, the driving force for step 2 in Fig. 8b is 0.36 eV larger than the driving force for the comparable step in free-base triad **3**, leading to extremely rapid electron transfer.

As the quantum yield of the initial charge-separated state in both triads is unity, the yield of the final $TTF^{\bullet+}$–P–$C_{60}^{\bullet-}$ state is determined by the partitioning of TTF–$P^{\bullet+}$–$C_{60}^{\bullet-}$ between charge recombination to the ground state (step 3) and charge shift from the TTF (step 4). For free-base triad **3**, the driving force for charge shift step 4 is 0.54 eV, and electron transfer is facile. The free energy change for recombination of TTF–$P_{2H}^{\bullet+}$–$C_{60}^{\bullet-}$ is so great, at −1.58 eV, that recombination is well into the Marcus inverted region where higher driving force leads to smaller rate constants. The result of these two factors is a high overall yield of charge separation, 87%. With zinc triad **4**, the driving force for charge shift is reduced to 0.34 eV, causing that reaction to be slower than in **3**. The free energy change for charge recombination, −1.41 eV, is smaller than it is for **3**, but since the reaction occurs in the inverted region, this implies a faster rate of charge recombination, as is observed (Table 1). These two factors work together to limit the yield of the final $TTF^{\bullet+}$–P_{Zn}–$C_{60}^{\bullet-}$ state to only 0.09.

Recombination of the $TTF^{\bullet+}$–P–$C_{60}^{\bullet-}$ state in the free-base or zinc porphyrins could in principle be either a direct, single-step process, or a two-step sequence wherein a rate-determining, endergonic recombination to TTF–$P^{\bullet+}$–$C_{60}^{\bullet-}$ is followed by rapid recombination *via* step 3. Charge recombination by the two-step process has been previously observed in some triad molecules, whereas in others, the one-step process, or a mixture of the two mechanisms, is observed.[13,14,43–45] Although the free energy difference between $TTF^{\bullet+}$–P_{2H}–$C_{60}^{\bullet-}$ and TTF–$P_{2H}^{\bullet+}$–$C_{60}^{\bullet-}$ is 0.20 eV larger than that between $TTF^{\bullet+}$–P_{Zn}–$C_{60}^{\bullet-}$ and TTF–$P_{Zn}^{\bullet+}$–$C_{60}^{\bullet-}$, the final charge-separated states of **3** and **4** have identical lifetimes in 2-methyltetrahydrofuran of 1.07 μs. This indicates that charge recombination occurs directly to the ground state (step 5 in Fig. 8), rather than *via* the two-step process. Similar behavior was noted for triads **1** and **2**.[15]

Comparison of tetrathiafulvalene and π-extended tetrathiafulvalene triads

Rate constants and free energy change values for the π-extended tetrathiafulvalene triads (**3**, **4**) and the previously studied tetrathiafulvalene triads (**1**, **2**) are reported in Table 1. In general, the excited state and redox properties of corresponding porphyrin and fullerene moieties in the two sets of triads are essentially identical. However, the π-extended tetrathiafulvalene moiety is more difficult to oxidize than the tetrathiafulvalene analog by ~0.06 V. (It should be realized that this value is only approximate, as the oxidation of the π-extended moieties is only quasireversible.) Qualitatively, the rate constants in Table 1 reflect this difference. Charge recombination of $TTF^{\bullet+}$–P_{Zn}–$C_{60}^{\bullet-}$ in **3** and **4** is a bit slower than it is in **1** and **2**. This is ascribed to a larger driving force for the reaction, which occurs in the Marcus inverted region. The charge shift reaction step 4 is faster for **1** than for **3**, and for **2** than for **4**, reflecting a slightly smaller driving force in the π-extended TTF triads for these reactions, which occur in the normal region of the Marcus–Hush relationship. Similarly, step 4 is faster for **1** than for **2**, and for **3** than for **4**, due to the larger driving force in the free base triads for these reactions, which also occur in the normal region.

Charge recombination to yield triplet states

A significant number of fullerene-containing dyad and triad molecules that demonstrate photoinduced electron transfer also feature charge recombination to yield a triplet state, rather than the ground state.[15] This sort of recombination requires an energetically accessible triplet, and is favored by the low reorganization energy for electron transfer characteristic of fullerenes. In triads **1**–**4**, recombination to yield a triplet is not observed, suggesting that the lowest-lying triplet states for all of the component chromophores are at significantly higher energy than the $TTF^{\bullet+}$–P–$C_{60}^{\bullet-}$ states. Thus, the lifetime of the final state is enhanced compared, for example, to triads of related structure and with similar energetics for electron transfer, but featuring carotenoid polyene electron donor moieties.

Conclusions

In summary, the π-extended tetrathiafulvalene investigated here exhibits many desirable characteristics as an electron donor moiety in supermolecular systems that demonstrate photoinduced electron transfer to yield long lived, energetic charge separated states in high quantum yield. Its first oxidation potential falls in a suitable range, its light absorption characteristics do not interfere with excitation of various visible-absorbing chromophores, and electronic coupling to the porphyrin is sufficiently strong that electron transfer from the tetrathiafulvalene to the porphyrin radical cation can compete with decay of the initial charge separated state to the ground state. In addition, the π-extended tetrathiafulvalene has nearly identical first and second oxidation potentials, which may make it a suitable two-electron donor in sequential multi-photon photoinduced electron transfer experiments. This last property could make these donor moieties important components of molecular-scale optoelectronic switches and logic gates.

Experimental

Instrumental techniques

The ^{1}H NMR spectra were recorded on Varian Unity spectrometers at 300 or 500 MHz. Unless otherwise specified, samples were dissolved in deuteriochloroform with tetramethylsilane as an internal reference. High resolution mass spectra were obtained on a Kratos MS 50 mass spectrometer operating at 8 eV in FAB mode. Other mass spectra were obtained on a matrix-assisted laser desorption/ionization time-of-flight spectrometer (MALDI-TOF). Ultraviolet–visible ground state absorption spectra were measured on a Shimadzu UV2100U UV–VIS spectrometer.

Steady state fluorescence emission spectra were measured using a Photon Technology International MP-1 and corrected. Excitation was produced by a 75 W xenon lamp and single grating monochromator. Fluorescence was detected at 90° to the excitation beam *via* a single grating monochromator and an R928 photomultiplier tube having S-20 spectral response operating in the single photon counting mode.

Fluorescence decay measurements were performed on ~1×10^{-5} M solutions by the single photon timing method, using an apparatus that has been previously described.[15,46]

Nanosecond transient absorption measurements were made with excitation from an Opotek optical parametric oscillator pumped by the third harmonic of a Continuum Surelight Nd : YAG laser (pulse width ~5 ns, repetition rate 10 Hz). The transient absorbance was measured using a diode detector equipped with 10 nm bandpass interference filters. The detection portion of the spectrometer has been described.[47]

The femtosecond transient absorption apparatus consisted of a kilohertz pulsed laser source and a pump–probe optical setup, as previously described.[15,48] To determine the number of lifetime components in the transient absorption data, singular value decomposition analysis was performed and decay-associated spectra derived, as previously described.[15]

Synthesis

The preparation of **1**, **2**, **5**, **9** and **10** has been previously reported.[15,35]

2-(*tert*-Butyldimethylsiloxymethyl)-9,10-anthraquinone (11). To a flask was added 2.0 g (8.4 mmol) of 2-(hydroxymethyl)-anthraquinone, 15 mL of DMF, 1.14 g (16.8 mmol) of imidazole and 1.90 g (12.6 mmol) of *tert*-butyldimethylsilyl chloride. The contents were stirred at room temperature in the dark and under a nitrogen atmosphere. After 24 h the reaction mixture was poured into diethyl ether (120 mL) and washed with water ($\times 5$). After drying the ether solution over Na_2SO_4, the solvent was evaporated and the crude product was chromatographed on silica gel (hexanes–15% ethyl acetate) to give 2.48 g of compound **11** (83% yield): ^{1}H NMR (300 MHz) δ 0.13 (6H, s, CH_3), 0.96 (9H, s, CH_3), 4.90 (2H, s, CH_2), 7.77–7.83 (3H, m, Ar-H), 8.24 (1H, s, Ar-H), 8.28–8.35 (3H, m, Ar-H); MALDI-TOF-MS *m*/*z* calcd for $C_{21}H_{24}O_3Si$ 353, obsd 354; UV–vis (CH_2Cl_2) 257, 277, 329 nm.

2-(*tert*-Butyldimethylsiloxymethyl)-9,10-bis(1,3-dithiol-2-ylidene)-9,10-dihydroanthracene (6). A flask containing 0.84 g (4.0 mmol) of dimethyl 1,3-dithiol-2-ylphosphonate[33,49] and 40 mL of THF was cooled to -78 °C under a nitrogen atmosphere. LDA (2.0 M/hexanes, 2.18 mL, 4.35 mmol) was added dropwise[50] and the resulting suspension was stirred for 1 h. Anthraquinone **11** (0.70 g, 1.98 mmol) was added as a solid, and the reaction mixture was stirred at -78 °C for 2 h followed by an additional 2 h at room temperature. The orange solution was concentrated and the residue redissolved in CH_2Cl_2, washed with water, dried over Na_2SO_4 and finally concentrated. The resulting material was chromatographed on silica gel (methylene chloride–hexanes; 2 : 1) to give 0.75 g of compound **6** (72% yield): ^{1}H NMR (300 MHz) δ 0.13 (6H, s, CH_3), 0.97 (9H, s, CH_3), 4.79 (2H, s, CH_2), 6.28 (4H, s, =C-H), 7.21–7.31 (3H, m, Ar-H), 7.63–7.72 (4H, m, Ar-H); MALDI-TOF-MS *m*/*z* calcd for $C_{27}H_{28}S_4OSi$ 525, obsd 525; UV–vis (CH_2Cl_2) 239, 270 (shoulder), 362, 426 nm.

2-(Hydroxymethyl)-9,10-bis(1,3-dithiol-2-ylidene)-9,10-dihydroanthracene (12). A flask containing 200 mg (0.38 mmol) of compound **6** and 20 mL of THF was cooled to -78 °C under a nitrogen atmosphere. Tetrabutylammonium fluoride (1 M in THF, 0.46 mL, 0.46 mmol) was added to the flask, and stirring was continued for 1 h at -78 °C followed by 1 h at room temperature. The reaction mixture was diluted with dichloromethane (100 mL), washed with water and then dried over Na_2SO_4. After evaporating the solvent at reduced pressure, the residue was chromatographed on silica gel (chloroform–3% methanol) to give 0.14 g of compound **12** (91% yield): ^{1}H NMR (300 MHz) δ 1.70 (1H, m, -OH), 4.74 (2H, d, $J = 4$ Hz, CH_2), 6.28 (4H, s, =C-H), 7.26–7.31 (3H, m, Ar-H), 7.66–7.71 (4H, m, Ar-H); MALDI-TOF-MS *m*/*z* calcd for $C_{21}H_{14}OS_4$ 410.6, obsd 410; UV–vis (CH_2Cl_2) 238, 270 (shoulder), 363, 428 nm.

Triad 3. A stirred suspension of 60 mg (0.04 mmol) of dyad **13**[15] in 8 mL of dichloromethane at 0 °C was treated with 7.0 μL (0.060 mmol) of *N*-methylmorpholine and 9.0 mg (0.051 mmol) of 2-chloro-4,6-dimethoxy-1,3,5-triazine. Stirring was continued at 0 °C for 10 min, and then at room temperature for 1 h. Portions of alcohol **12** (16 mg, 0.040 mmol) and 4-dimethylaminopyridine (10 mg, 0.079 mmol) were added. After 1 h the solvent was evaporated and the residue was chromatographed on silica gel (toluene–carbon disulfide–ethyl acetate, 65 : 33 : 2) to give 66 mg of triad **3** (85% yield): ^{1}H NMR (300 MHz, $CDCl_3$–CS_2 2 : 1) δ -2.72 (2H, s, NH), 1.77 (6H, s, Ar-CH_3), 1.79 (6H, s, Ar-CH_3), 2.58 (6H, s, Ar-CH_3), 3.11 (3H, s, N-CH_3), 4.42 (1H, d, $J = 9$ Hz, pyrrolid-H), 5.09 (1H, d, $J = 9$ Hz, pyrrolid-H), 5.26 (1H, s, pyrrolid-H), 5.54 (2H, s, CH_2), 6.24 (1H, s, =C-H), 6.25 (1H, s, =C-H), 6.27 (2H, s, =C-H), 7.10 (1H, d, $J = 7$ Hz, anthr-H), 7.20 (4H, s, Ar-H), 7.22–7.24 (1H, m, anthr-H), 7.42 (1H, dd, $J = 8$ Hz, 2 Hz, anthr-H), 7.62 (1H, t, $J = 3$ Hz, anthr-H), 7.64 (1H, t, $J = 3$ Hz, anthr-H), 7.70 (1H, d, $J = 8$ Hz, anthr-H), 7.85 (1H, d, $J = 2$ Hz, anthr-H), 8.17 (2H, br s, Ar-H), 8.24 (2H, d, $J = 5$ Hz, Ar-H), 8.26 (2H, d, $J = 5$ Hz, Ar-H), 8.46 (2H, d, $J = 5$ Hz, Ar-H), 8.60 (4H, br s, β-H), 8.63 (2H, d, $J = 3$ Hz, β-H), 8.69 (2H, d, $J = 3$ Hz, β-H); FAB-MS calcd for $C_{135}H_{59}N_5O_2S_4$ 1909.3552, obsd 1910.3600 $(M + H)^+$; UV–vis (CH_2Cl_2) 241, 365, 422, 516, 550, 592, 648, 708 nm.

Triad 4. As needed, a small portion of **3** in dichloromethane and an excess of zinc acetate were stirred, and **4** was isolated in essentially quantitative yield by TLC (silica gel); MALDI-TOF-MS *m*/*z* calcd for $C_{135}H_{57}N_5O_2S_4Zn$ 1975, obsd 1976; UV–vis (CH_2Cl_2) 248, 310, 420, 514, 550, 590, 704 nm.

Dyad 7. A solution of 60 mg (0.075 mmol) of porphyrin **14**[15] and 16 μL (0.15 mmol) of *N*-methylmorpholine in 8 mL of dichloromethane at 0 °C was treated with 17 mg (0.097 mmol) of 2-chloro-4,6-dimethoxy-1,3,5-triazine. Stirring was continued at 0 °C for 10 min and then at room temperature for 2.5 h. Alcohol **12** (30 mg, 0.075 mmol) and 19 mg (0.156 mmol) of 4-dimethylaminopyridine were added to the reaction mixture. After 30 min the solvent was evaporated and the residue was chromatographed on silica gel (toluene–1% ethyl acetate) to give 68 mg of dyad **7** (76% yield): ^{1}H NMR (500 MHz) δ -2.62 (2H, s, NH), 1.84 (12H, s, Ar-CH_3), 2.62 (6H, s, Ar-CH_3), 4.16 (3H, s, -$COOCH_3$), 5.62 (2H, s, CH_2), 6.30 (1H, s, =C-H), 6.32 (3H, s, =C-H), 7.19 (1H, d, $J = 8$ Hz, anthr-H), 7.30 (4H, s, Ar-H), 7.32 (1H, m, anthr-H), 7.51 (1H, d, $J = 8$ Hz, anthr-H), 7.73 (2H, br s, anthr-H), 7.81 (1H, d, $J = 8$ Hz, anthr-H), 7.97 (1H,s, anthr-H), 8.32 (4H, d, $J = 8$ Hz, Ar-H), 8.44 (2H, d, $J = 8$ Hz, Ar-H), 8.51 (2H, d, $J = 8$ Hz, Ar-H), 8.74 (8H, m, β-H); MALDI-TOF-MS *m*/*z* calcd for $C_{74}H_{56}N_4O_4S_4$ 1194, obsd 1194; UV–vis (CH_2Cl_2) 239, 368, 414, 516, 550, 592, 648 nm.

Dyad 8. As needed, a small portion of dyad **7** in dichloromethane and an excess of zinc acetate were stirred, and **8** was isolated in essentially quantitative yield by TLC (silica gel); MALDI-TOF-MS *m*/*z* calcd for $C_{74}H_{54}N_4O_4S_4Zn$ 1257, obsd 1258; UV–vis (CH_2Cl_2) 313, 422, 550, 592 nm.

Acknowledgement

This work was supported by a grant from the National Science Foundation (CHE-0078835). FAB mass spectrometric studies were performed by the Midwest Center for Mass Spectrometry, with partial support by the National Science Foundation (DIR9017262). This is publication 503 from the ASU Center for the Study of Early Events in Photosynthesis.

References

1 D. Gust, T. A. Moore and A. L. Moore, *Acc. Chem. Res.*, 2001, **34**, 40.
2 M. Bixon, J. Fajer, G. Feher, J. H. Freed, D. Gamliel, A. J. Hoff, H. Levanon, K. Möbius, R. Nechushtai, J. R. Norris, A. Scherz, J. L. Sessler and D. Stehlik, *Isr. J. Chem.*, 1992, **32**, 449.
3 D. Gust and T. A. Moore, in *The Porphyrin Handbook*, ed. K. M. Kadish, K. M. Smith, and R. Guilard, Academic Press, New York, 2000, p. 153.
4 Y. Sakata, H. Imahori, H. Tsue, S. Higashida, T. Akiyama, E. Yoshizawa, M. Aoki, K. Yamada, K. Hagiwara, S. Taniguchi and T. Okada, *Pure Appl. Chem.*, 1997, **69**, 1951.
5 M. R. Wasielewski, *Chem. Rev.*, 1992, **92**, 435.
6 D. Gust, T. A. Moore and A. L. Moore, *IEEE Eng. Med. Biol.*, 1994, **13**, 58.
7 P. A. Liddell, J. P. Sumida, A. N. Macpherson, L. Noss,

G. R. Seely, K. N. Clark, A. L. Moore, T. A. Moore and D. Gust, *Photochem. Photobiol.*, 1994, **60**, 537.
8 H. Imahori, K. Hagiwara, M. Aoki, T. Akiyama, S. Taniguchi, T. Okada, M. Shirakawa and Y. Sakata, *J. Am. Chem. Soc.*, 1996, **118**, 11771.
9 H. Imahori, K. Hagiwara, T. Akiyama, M. Aoki, S. Taniguchi, T. Okada, M. Shirakawa and Y. Sakata, *Chem. Phys. Lett.*, 1996, **263**, 545.
10 D. M. Guldi and K.-D. Asmus, *J. Am. Chem. Soc.*, 1997, **119**, 5744.
11 S. Larsson, A. Klimkans, L. Rodriguez-Monge and G. Duskesas, *J. Mol. Struct.*, 1998, **425**, 155.
12 P. A. Liddell, D. Kuciauskas, J. P. Sumida, B. Nash, D. Nguyen, A. L. Moore, T. A. Moore and D. Gust, *J. Am. Chem. Soc.*, 1997, **119**, 1400.
13 D. Kuciauskas, P. A. Liddell, S. Lin, S. Stone, A. L. Moore, T. A. Moore and D. Gust, *J. Phys. Chem. B*, 2000, **104**, 4307.
14 J. L. Bahr, D. Kuciauskas, P. A. Liddell, A. L. Moore, T. A. Moore and D. Gust, *J. Photochem. Photobiol.*, 2000, **72**, 598.
15 P. A. Liddell, G. Kodis, L. de la Garza, J. L. Bahr, A. L. Moore, T. A. Moore and D. Gust, *Helv. Chim. Acta*, 2001, **84**, 2765.
16 P. R. Ashton, V. Balzani, J. Becher, A. Credi, M. C. T. Fyfe, G. Mattersteig, S. Menzer, M. B. Nielsen, F. M. Raymo, J. F. Stoddart, M. Venturi and D. J. Williams, *J. Am. Chem. Soc.*, 1999, **121**, 3951.
17 M. A. Herranz, B. Illescas, N. Martin, C. P. Luo and D. M. Guldi, *J. Org. Chem.*, 2000, **65**, 5728.
18 N. Martin, L. Sanchez, M. A. Herranz and D. M. Guldi, *J. Phys. Chem. A*, 2000, **104**, 4648.
19 M. A. Herranz, N. Martin, L. Sanchez, C. Seoane and D. M. Guldi, *J. Organomet. Chem.*, 2000, **599**, 2.
20 M. Prato, M. Maggini, C. Giacometti, G. Scorrano, G. Sandona and G. Farnia, *Tetrahedron*, 1996, **52**, 5221.
21 N. Martin, L. Sanchez, C. Seoane, R. Andreu, J. Garin and J. Orduna, *Tetrahedron Lett.*, 1996, **37**, 5979.
22 N. Martin, I. Perez, L. Sanchez and C. Seoane, *J. Org. Chem.*, 1997, **62**, 5690.
23 C. Boulle, J. M. Rabreau, P. Hudhomme, M. Cariou, M. Jubault, A. Gorgues, J. Orduna and J. Garin, *Tetrahedron Lett.*, 1997, **38**, 3909.
24 M. R. Bryce, *Adv. Mater.*, 1999, **11**, 11.
25 J. Llacay, J. Veciana, J. Vidal-Gancedo, J. L. Bourdelande, R. Gonzalez-Moreno and C. Rovira, *J. Org. Chem.*, 1998, **63**, 5201.
26 J. Llacay, M. Mas, E. Molins, J. Veciana, D. Powell and C. Rovira, *Chem. Commun.*, 1997, 659.
27 M. R. Bryce, *J. Mater. Chem.*, 2000, **10**, 589.
28 D. M. Guldi, S. Gonzalez, N. Martin, A. Anton, J. Garin and J. Orduna, *J. Org. Chem.*, 2000, **65**, 1978.
29 S.-G. Liu, I. Perez, N. Martin and L. Echegoyen, *J. Org. Chem.*, 2000, **65**, 9092.
30 M. Maggini, G. Scorrano and M. Prato, *J. Am. Chem. Soc.*, 1993, **115**, 9798.
31 E. Cerrada, M. R. Bryce and A. J. Moore, *J. Chem. Soc., Perkin Trans. 1*, 1993, 5373.
32 M. A. Herranz, S. Gonzalez, I. Perez and N. Martin, *Tetrahedron*, 2001, **57**, 725.
33 A. J. Moore and M. R. Bryce, *J. Chem. Soc., Perkin Trans. 1*, 1991, 157.
34 D. Kuciauskas, S. Lin, G. R. Seely, A. L. Moore, T. A. Moore, D. Gust, T. Drovetskaya, C. A. Reed and P. D. W. Boyd, *J. Phys. Chem.*, 1996, **100**, 15926.
35 G. Kodis, P. A. Liddell, L. de la Garza, P. C. Clausen, J. S. Lindsey, A. L. Moore, T. A. Moore and D. Gust, *J. Phys. Chem. A*, 2002, **106**, 2036.
36 G. H. Golub and C. Reinsch, *Numer. Math.*, 1970, **14**, 403.
37 E. R. Henry and J. Hofrichter, in *Methods in Enzymology*, ed. B. Ludwig, Academic Press, San Diego, 1992, p. 219.
38 A. E. Jones, C. A. Christensen, D. F. Perepichka, A. S. Batsanov, A. Beeby, P. J. Low, M. R. Bryce and A. W. Parker, *Chem. Eur. J.*, 2001, **7**, 973.
39 R. A. Marcus, *J. Chem. Phys.*, 1956, **24**, 966.
40 R. A. Marcus, *Pure Appl. Chem.*, 1997, **69**, 13.
41 N. S. Hush, *J. Chem. Phys.*, 1958, **28**, 962.
42 N. S. Hush, *Trans. Faraday Soc.*, 1961, **57**, 557.
43 D. Gust, T. A. Moore, L. R. Makings, P. A. Liddell, G. A. Nemeth and A. L. Moore, *J. Am. Chem. Soc.*, 1986, **108**, 8028.
44 M. Ohkouchi, A. Takahashi, N. Mataga, T. Okada, A. Osuka, H. Yamada and K. Maruyama, *J. Am. Chem. Soc.*, 1993, **115**, 12137.
45 A. Osuka, H. Yamada, T. Shinoda, K. Nozaki and O. Ohno, *Chem. Phys. Lett.*, 1995, **238**, 37.
46 D. Gust, T. A. Moore, D. K. Luttrull, G. R. Seely, E. Bittersmann, R. V. Bensasson, M. Rougée, E. J. Land, F. C. de Schryver and M. Van der Auweraer, *Photochem. Photobiol.*, 1990, **51**, 419.
47 F. S. Davis, G. A. Nemeth, D. M. Anjo, L. R. Makings, D. Gust and T. A. Moore, *Rev. Sci. Instrum.*, 1987, **58**, 1629.
48 A. Freiberg, K. Timpmann, S. Lin and N. W. Woodbury, *J. Phys. Chem. B*, 1998, **102**, 10974.
49 F. Wudl and M. L. Kaplan, *J. Org. Chem.*, 1974, **39**, 3608.
50 N. Godert, A. S. Batsanov, M. R. Bryce and J. A. K. Howard, *J. Org. Chem.*, 2001, **66**, 713.